The 2018 International Conference On Control Automation & Information Sciences (ICCAIS 2018)
October 24-27, 2018, Hangzhou, China.

δ-Generalised Labelled Multi-Bernoulli Simultaneous Localisation and Mapping

Diluka Moratuwage and Martin Adams
Dept. of Electrical Engineering & Advanced Mining Technology Center
Universidad de Chile
Santiago, Chile
Email: dmoratuwage@ing.uchile.cl, martin@ing.uchile.cl

Felipe Inostroza
Dept. of Electrical Engineering
Universidad de Chile
Santiago, Chile
Email: finostro@ug.uchile.cl

***Abstract*—Motivated by the need for simultaneous localisation and mapping (SLAM) algorithms which circumvent the requirement of external data association routines and map management heuristics, and account for realistic sensor detection uncertainty, recent literature has adopted Random Finite Set (RFS) based approaches. Solutions based on the Probability Hypothesis Density (PHD) filter and more recently the Labelled Multi-Bernoulli (LMB) filter have been demonstrated. The LMB filter was introduced as an efficient approximation of the computationally expensive δ-Generalised LMB (δ-GLMB) filter. The LMB filter converts its representation of an LMB distribution to δ-GLMB form and back during the measurement update step. This conversion results in a loss of information and in general yields inferior results compared to the δ-GLMB filter. To address this issue, we present a SLAM solution using an efficient variant of the δ-GLMB filter (δ-GLMB-SLAM) based on Gibbs sampling, which is computationally comparable to LMB-SLAM, yet more accurate and robust against sensor noise, measurement clutter and feature detection uncertainty. The performance of the proposed δ-GLMB-SLAM algorithm is compared to the LMB-SLAM algorithm with a Gibbs sampling based joint map prediction and update approach using a series of simulations.**

***Index Terms*—SLAM, robotics, tracking, random finite sets**

I. Introduction

Simultaneous localisation and mapping (SLAM) is the process of incrementally building a map of the environment using data from noisy sensors (exteroceptive and proprioceptive) mounted on a mobile robot and estimating the robot's position over time with respect to this map. SLAM is considered as an integral process required by many mobile robotic applications.

Starting from the seminal work of Smith et al. in [1], many improvements have been proposed to the estimation theoretic SLAM problem. In [2] Dissanayake et al. proposed an extended Kalman Filter based SLAM (EKF-SLAM) solution. In [3] the FastSLAM algorithm was proposed, which adopts the concept of a Rao-Blackwellized particle filter. In [4], an extended information filter based SLAM (EIF-SLAM) algorithm was proposed as an alternative to EKF-SLAM with improved computational requirements. In recent years, SLAM has been modelled as a factor graph [5] and solved as a maximum a posterior (MAP) estimation problem. Some of the original contributions under this paradigm include [6] [7]. Although such methods in general produce superior results, they still inherit several fundamental problems [8]. One such problem is the heuristic based data association phase, which can affect the optimization and severely degrade the performance of the algorithm. Also, the accuracy of these solutions relies on the assumption that the environment is static, which may produce inferior results in challenging dynamic environments. This article proposes that the above mentioned issues can be efficiently addressed using the recent RFS filtering framework.

In both the estimation theoretic and optimisation based SLAM paradigms, robot position, landmark map and the measurements are traditionally represented as random vectors. Representing the landmark map, and measurements as random vectors requires solutions to additional sub-problems such as finding measurement to landmark associations, clutter (false measurements) removal and map management before applying the Bayes recursion or optimisation.

Parallel to developments in SLAM, Mahler [9] proposed to represent a multi-target state by a finite set in Bayesian multi-target tracking as it caters for a mathematically consistent notion of estimation error. Mahler further devised a set of mathematical tools called finite set statistics (FISST) using integration and probability density for characterizing a random finite set (RFS), which is consistent with point process theory [10]. The RFS representation of the multi-object state can cater for target detection uncertainty, data association uncertainty and clutter filtering that are common in real-world target tracking applications. Mahler further devised the Probability Hypothesis Density (PHD) filter [11], Cardinalized PHD (CPHD) filter [12] and the multi-Bernoulli filter [9] as tractable approximations to the optimal Bayesian multi-target filter. More recently in [13] [14] Vo et al. introduced the δ-Generalized Labelled multi-Bernoulli (δ-GLMB) filter as an analytic solution to the multi-target Bayes recursion. In [15], Reuter et al. proposed the Labeled multi-Bernoulli (LMB) filter as an efficient approximation to the more computationally expensive δ-GLMB filter. In [16], Vo et al. introduced an efficient implementation of the δ-GLMB filter by combining the prediction and update steps and introducing a truncation approach using Gibbs sampling.

The similarities between multi-target tracking and SLAM led to the adoption of RFS modeling of landmark map and measurements in SLAM. In [17] Mullane et al. presented the first SLAM formulation using RFSs and later they pro-

978-1-5386-6020-1/18/$31.00 ©2018 IEEE

posed improved SLAM solutions based on Rao-Blackwellized particle filtering in [18] and [19]. Although the PHD-SLAM solution is robust against noisy sensory information and measurement clutter, it models the landmark map as a Poisson distributed RFS. In [20], an improved solution to the SLAM problem was proposed by propagating the landmark map using a Labeled Multi-Bernoulli (LMB) filter (named LMB-SLAM), where a landmark is represented not only by its kinematic state but also by a label. Such a representation may be beneficial for filter based SLAM solutions with semantic features, especially during loop closure detection. Furthermore, labeled features provide a convenient identification and classification method for SLAM algorithms having multiple feature types (see [21] for a recent approach that may benefit from labeled features).

Unlike PHD-SLAM, which assumes the landmark map is a Poisson distributed RFS, LMB-SLAM makes no assumptions about the map and in general produces superior performance. However, the LMB filter internally converts its LMB representation of the map to a δ-GLMB distribution and back to an LMB distribution during the measurement update step, yielding a loss of information and hence accuracy (see [22] for comparisons). Moreover, the performance of the LMB-SLAM filter depends on the partitioning of landmarks present in the sensor field of view (FOV) [22]. If the landmarks are easily separable into partitions, LMB-SLAM performs efficiently. On the other hand if the landmarks are not easily separable into partitions, the computational cost is equivalent to employing a δ-GLMB filter. Although in multi-target tracking, closely spaced targets are not common, in SLAM it is highly likely to encounter clustered and unevenly distributed landmarks which appear in the sensor FOV. Furthermore, feature extraction algorithms may produce multiple closely spaced features (for example when using low resolution lidar), which may result in possible performance degradation in LMB-SLAM.

In a manner similar to PHD-SLAM and LMB-SLAM, in this article, we rely on the Rao-Blackwellized particle filter for robot trajectory estimation but adopt the recently developed efficient δ-GLMB filter [16] for landmark map estimation. The proposed algorithm, called δ-GLMB-SLAM inherits the joint prediction/update method of the efficient δ-GLMB filter [16] for landmark map posterior propagation. Furthermore, the Gibbs sampling based truncation approach [16] results in large computational savings compared to the original δ-GLMB filter [13] [14]. Using a series of simulations, it is shown that the proposed δ-GLMB-SLAM solution, outperforms LMB-SLAM in terms of pose estimation error, quality of the map and running time yielding robust performance under varying clutter conditions and feature detection uncertainty.

II. Problem Formulation

Let $\mathbf{u}_{1:k} = [\mathbf{u}_1, \mathbf{u}_2, \ldots, \mathbf{u}_k]^T$ denote the time sequence of control commands applied to the robot up to time k, where $\mathbf{u}_k$ denotes the control command applied at time k. Let the time sequence of the pose history of the robot be denoted by $\mathbf{x}_{1:k} = [\mathbf{x}_1, \mathbf{x}_2, \ldots, \mathbf{x}_k]^T$, where $\mathbf{x}_k$ denotes the pose of the robot with respect to the global frame of reference at time k. Let the time sequence of sets of measurements obtained using an exteroceptive sensor mounted on the vehicle be denoted by $\mathcal{Z}_{1:k} = [\mathcal{Z}_1, \mathcal{Z}_2, \ldots, \mathcal{Z}_k]$, where $\mathcal{Z}_k = \{\mathbf{z}_{k,1}, \mathbf{z}_{k,2}, \ldots, \mathbf{z}_{k,m_k}\}$ denotes the measurement detection set received at time k, where m_k denotes the number of detections.

A. Labelled RFS representation of the Map

Let the landmark map be represented as a labeled RFS $\mathcal{M} = \{\hat{\mathbf{m}}_{k,1}, \hat{\mathbf{m}}_{k,2}, \ldots, \hat{\mathbf{m}}_{k,n_k}\}$ where n_k denotes the number of estimated landmarks at time k. Each realisation of a landmark $\hat{\mathbf{m}} \in \mathcal{M}$ is of the form $\hat{\mathbf{m}} = (\mathbf{m}, l)$, where $\mathbf{m} \in \mathbb{M}$ is the kinematic state and $l \in \mathbb{L}$ is a distinct label of the point $\mathbf{m}$. Distinct labels provide a method to distinguish between landmarks [13] [14].

Let the kinematic state space of a landmark be denoted by $\mathbb{M}$ and the discrete label space be denoted by $\mathbb{L}$. Further, let $\mathcal{L} : \mathbb{M} \times \mathbb{L} \to \mathbb{L}$ be the projection from labeled RFSs to labels defined by $\mathcal{L}(\mathbf{m}, l) = l$. Let the Kronecker delta function for arbitrary arguments (such as vectors, sets or integers) be denoted by $\delta_{\mathcal{Y}}(\mathcal{X})$, which takes the value of 1 only if $\mathcal{X} = \mathcal{Y}$ and 0 otherwise. The indicator function $1_{\mathcal{X}}(\mathcal{Y})$ takes the value of 1 if $\mathcal{Y} \in \mathcal{X}$ and 0 otherwise. Let $\Delta(\mathcal{M}) \triangleq \delta_{|\mathcal{M}|}(|\mathcal{L}(\mathcal{M})|)$ denote the distinct label indicator, which takes the value of 1 if and only if the labeled set $\mathcal{M}$ has the same cardinality as its labels $\mathcal{L}(\mathcal{M}) = \{\mathcal{L}(\hat{\mathbf{m}}) : \hat{\mathbf{m}} \in \mathcal{M}\}$ and 0 otherwise. Let $\mathcal{F}(\mathcal{J})$ represent all finite subsets of a set $\mathcal{J}$. The inner product of two continuous functions is denoted by $\langle f, g \rangle \triangleq \int f(\mathbf{x}) g(\mathbf{x}) d\mathbf{x}$ and for a real valued function $h(\mathbf{x})$, the multi-object exponential is defined as $h(\cdot)^{\mathcal{X}} \triangleq \prod_{\mathbf{x} \in \mathcal{X}} h(\mathbf{x})$.

B. Rao-Blackwellization of the SLAM problem

In the SLAM problem, it is required to evaluate the posterior probability distribution,

$$p_{k|k}(\mathcal{M}_k, \mathbf{x}_{1:k} | \mathcal{Z}_{1:k}, \mathbf{u}_{1:k}, \mathbf{x}_0) \tag{1}$$

for all times k, where $\mathbf{x}_0$ denotes the initial pose of the vehicle. In other words, it is required to evaluate the joint posterior density consisting of the map and the robot pose history at all times k, given the time sequences of sets of observations, and control commands up to and including time k and the initial robot pose.

The joint posterior density consisting of the landmark map $\mathcal{M}_k$ and robot trajectory $\mathbf{x}_{1:k}$ at time k, is evaluated using the existing map $\mathcal{M}_{k-1}$, history of robot poses $\mathbf{x}_{0:k-1}$ evaluated at time $k-1$, the time sequence of sets of observations $\mathcal{Z}_{1:k}$ and the applied control commands $\mathbf{u}_{1:k}$ up to and including time k. In a manner similar to Montemerlo's approach in FastSLAM [3], we factorise the SLAM posterior into a product of the robot trajectory posterior and the map posterior conditioned on the robot trajectory as follows,

$$\begin{aligned} &p_{k|k}(\mathcal{M}_k, \mathbf{x}_{1:k} | \mathcal{Z}_{1:k}, \mathbf{u}_{1:k}, \mathbf{x}_0) \\ &= p_{k|k}(\mathcal{M}_k | \mathcal{Z}_{1:k}, \mathbf{x}_{0:k}) \\ &\times p_{k|k}(\mathbf{x}_{1:k} | \mathcal{Z}_{1:k}, \mathbf{u}_{1:k}, \mathbf{x}_0) \end{aligned} \tag{2}$$

This decouples the SLAM problem into two separate (conditionally dependant) estimation problems. The key advantage

of this factorisation is two-fold, firstly it can benefit from using Monte Carlo methods (particle filtering) for joint robot trajectory estimation, making it possible to adopt complex non-linear motion models. Secondly, it can benefit from using an RFS representation and FISST techniques for landmark map posterior estimation. By representing the map and measurements as RFSs and appropriately modelling the map transition model, it is possible to estimate multiple landmarks in the presence of measurement noise and clutter by implicitly taking data association, landmark detection and landmark survival uncertainties into account within a single joint estimation framework.

C. δ-GLMB-SLAM Observation Model

The measurement set received from the onboard sensor at time k contains both landmark generated measurements and false alarms (measurement clutter). Let the RFS $\mathcal{C}_k$ denote the measurement clutter, then the measurements received at time k can be modelled by the RFS,

$$\mathcal{Z}_k = \mathcal{C}_k \cup \left[\bigcup_{(\mathbf{m}_k, l_k) \in \mathcal{M}_k} \mathcal{H}_k(\mathbf{m}_k, l_k) \right] \tag{3}$$

where, $\mathcal{H}_k(\mathbf{m}_k, l_k)$ is a Bernoulli RFS representing the measurement corresponding to the observation of landmark $(\mathbf{m}_k, l_k) \in \mathcal{M}_k$. Due to the limited field of view (FOV) of the sensor $\mathcal{H}_k(\mathbf{m}_k, l_k)$ can have a value of the form $\{\mathbf{z}_k\}$ with probability of detection $p_{\mathbf{D}}(\mathbf{m}_k, l_k|\mathbf{x}_k)$ or $\emptyset$ with probability of $1 - p_{\mathbf{D}}(\mathbf{m}_k, l_k|\mathbf{x}_k)$. Note that probability of detection is a function of landmark state and robot position. The measurement likelihood function conditioned on the detection of the landmark with state $(\mathbf{m}_k, l_k)$ is given by $g_k(\mathbf{z}_k|\mathbf{m}_k, l_k, \mathbf{x}_k)$. Assuming that the measurements are conditionally independent and the measurement clutter is an independent process, the measurement likelihood function corresponding to the observations can be written as,

$$g(\mathcal{Z}|\mathcal{M}, \mathbf{x}) = \mathbf{e}^{-\langle \kappa, \mathbf{1} \rangle} \kappa^{\mathcal{Z}} \sum\nolimits_{\theta \in \Theta(\mathcal{L}(\mathcal{M}))} [\psi_{\mathcal{Z}}(\cdot; \theta)]^{\mathcal{M}} \tag{4}$$

where κ denotes the intensity of Poisson distributed measurement clutter and,

$$\psi_{\mathcal{Z}}(\mathbf{m}, l; \theta) = \begin{cases} \frac{p_{\mathbf{D}}(\mathbf{m}, l) g(\mathbf{z}_{\theta(l)}|\mathbf{m}, l, \mathbf{x})}{\kappa(\mathbf{z}_{\theta(l)})} & \text{if } \theta(l) > 0 \\ 1 - p_{\mathbf{D}}(\mathbf{m}, l) & \text{if } \theta(l) = 0 \end{cases} \tag{5}$$

where θ is an association map of the form, $\theta : \mathbb{L} \to 0, 1, \ldots, |\mathcal{Z}|$ such that each distinct estimated feature is associated to a distinct measurement (i.e. $\theta(i) = \theta(i') > 0$ implies $i = i'$). The set Θ of all such association maps is called the association map space and a subset of association maps with domain $\mathcal{I}$ is denoted by $\Theta(\mathcal{I})$. Note that, unlike multi-target tracking, in SLAM, already estimated landmarks that exit the current sensor FOV are retained in the map with probability of detection $p_{\mathbf{D}}(\mathbf{m}, l) = 0$ during the measurement update step and therefore in general contribute to the robot trajectory posterior estimate.

D. δ-GLMB-SLAM Map transition model

As the robot continues to explore the unknown environment, new observations are collected in the limited FOV of the sensor and fused into the landmark map. These new landmarks are modelled as the labelled RFS $\mathcal{Q}_k$ with the birth label space $\mathbb{B}$, and the corresponding birth density is assumed to be a labelled multi-Bernoulli density of the form,

$$f_B(\mathcal{Q}_k) = \Delta(\mathcal{Q})[1 - r_B^{(\cdot)}]^{\mathbb{B} - \mathcal{L}(\mathcal{Q}_k)} [1_{\mathbb{B}}(\cdot) r_B^{(\cdot)}]^{\mathcal{L}(\mathcal{Q}_\mathbf{k})} [p_B]^{\mathcal{Q}_k} \tag{6}$$

where a realisation of $r_B^{(\cdot)}$ is of the form $r_B^{(l)} = r_B(\mathbf{m}, l)$ for any label $l \in \mathbb{B} - \mathcal{L}(\mathcal{Q}_k)$ and denotes the birth probability of the landmark with label l and $p_B(\mathbf{m}, l)$ denotes its spatial distribution.

Furthermore, a portion of the already existing landmarks in the map appears in the current sensor FOV. Given the state of the current landmark map, $\mathcal{M}$, a landmark $(\mathbf{m}_k, l_k) \in \mathcal{M}$ may appear in the sensor FOV in the next time step with probability $p_S(\mathbf{m}, l)$ and change its state to $(\mathbf{m}_{k+1}, l_{k+1})$ with probability density $\delta_{\mathbf{m}_k}(\mathbf{m}_{k+1}) \delta_{l_k}(l_{k+1})$, or leave the sensor FOV with probability $q_S(\mathbf{m}, l) = 1 - p_S(\mathbf{m}, l)$. It is important to note that unlike multi-target tracking, in SLAM, landmarks are usually assumed stationary and hence the motion of a landmark is modelled as a Kronecker delta function, $\delta_{\mathbf{m}_k}(\mathbf{m}_{k+1})$. In addition, the label of a landmark is preserved during the state transition. Assuming that the state of the landmark map is represented by $\mathcal{M}$, the set of surviving landmarks in the next time step is modelled as a labeled multi-Bernoulli (LMB) RFS $\mathcal{W}$ with parameter set $\{(p_S(\mathbf{m}, l), \delta_{\mathbf{m}}(\cdot)\delta_l(\cdot)) : (\mathbf{m}, l) \in \mathcal{M}\}$. The state transition is modelled as a LMB distribution given by,

$$f_S(\mathcal{W}|\mathcal{M}) = \Delta(\mathcal{W})\Delta(\mathcal{M}) 1_{\mathcal{L}(\mathcal{M})}(\mathcal{L}(\mathcal{W}))[\Phi(\mathcal{W}; \cdot)]^{\mathcal{M}}, \tag{7}$$

where,

$$\begin{aligned} \Phi(\mathcal{W}; \mathbf{m}_{k+1}, l_{k+1}) = & \sum_{(\mathbf{m}_{k+1}, l_{k+1}) \in \mathcal{W}} \delta_{l_k}(l_{k+1}) p_S(\mathbf{m}_k, l_k) \delta_{\mathbf{m}_k}(\mathbf{m}_{k+1}) \\ & + [1 - 1_{\mathcal{L}(\mathcal{W})}(l_k)] q_S(\mathbf{m}_k, l_k). \end{aligned} \tag{8}$$

The newly appearing (birth) landmarks are independent of the already existing landmarks in the map. Therefore, it can be shown that the probability density of the predicted state of the map $\mathcal{M}_{k+1}$ conditioned on the current map $\mathcal{M}_k$ can be written as a product of birth density and the transition density of the surviving landmarks as follows [13],

$$\begin{aligned} f(\mathcal{M}_{k+1}|\mathcal{M}_k) = & f_S(\mathcal{M}_{k+1} \cap (\mathbb{M} \times \mathbb{L})|\mathcal{M}_k) \\ & \times f_B(\mathcal{M}_{k+1} - (\mathbb{M} \times \mathbb{L})). \end{aligned} \tag{9}$$

Note that, the estimated landmarks that exit the current sensor FOV should remain in the map and be modelled with probability of survival $p_S(\mathbf{m}, l) = 1$ during the prediction step and contribute to the robot trajectory posterior estimation.

E. δ-GLMB-SLAM Map Estimation

To propagate the landmark map in time, we adopt the recently proposed efficient δ-GLMB filter [16]. This approach

978-1-5386-6020-1/18/$31.00 ©2018 IEEE

avoids the traditional prediction/update steps of a filter and directly updates the posterior at time k to time $k+1$, achieving significant computational savings. Let the map posterior at time k, $p(\mathcal{M}_k|\mathcal{Z}_{1:k}, \mathbf{x}_{0:k})$ be abbreviated as $p(\mathcal{M})$ and let the measurement updated landmark map posterior at time $k+1$ be abbreviated as $p(\mathcal{M}_+|\mathcal{Z}_+)$. Assume that $p(\mathcal{M})$ at time k is given by the δ-GLMB distribution of the following form,

$$p(\mathcal{M}) = \Delta(\mathcal{M}) \sum_{(\mathcal{I},\xi)\in\mathcal{F}(\mathbb{L})\times\Xi} \omega^{(\mathcal{I},\xi)}\delta_{\mathcal{I}}(\mathcal{L}(\mathcal{M}))[p^{(\xi)}]^{\mathcal{M}}, \tag{10}$$

where $\mathcal{I} \in \mathcal{F}(\mathbb{L})$ represents a set of landmark labels and $\xi \in \Xi$ represents a history of association maps upto time k and denoted by $\xi = (\theta_1, ..., \theta_k)$. The pair $(\mathcal{I}, \xi)$ represents the hypothesis that the set of landmarks $\mathcal{I}$ has history ξ of association maps and the weight $\omega^{(\mathcal{I},\xi)}$ represents the probability of the hypothesis $(\mathcal{I}, \xi)$ and $p^{(\xi)}(\mathbf{m}, l)$ represents the probability density of the kinematic state of the feature with label l and the association map history ξ.

Assume that the birth landmarks (newly appearing landmarks) and the surviving landmarks in the FOV follow labeled multi-Bernoulli distributions. Let $\mathbb{B}_+$ denote the label space of newly appearing features in the FOV at time $k+1$. Then, adopting the joint prediction/update approach proposed in [16], the measurement updated map posterior $p(\mathcal{M}_+|Z_+)$ can be written as,

$$\begin{aligned} p(\mathcal{M}_+|\mathcal{Z}_+) \propto \Delta(\mathcal{M}_+) \sum_{\mathcal{I},\xi,\mathcal{I}_+,\theta_+} & \bar{\omega}_{Z_+}^{(\mathcal{I},\xi,\mathcal{I}_+,\theta_+)} \\ & \times \delta_{\mathcal{I}_+}(\mathcal{L}(\mathcal{M}_+))[p_{\mathcal{Z}_+}^{(\xi,\theta_+)}]^{\mathcal{M}_+}, \end{aligned} \tag{11}$$

where $\mathbb{L}_+ = \mathbb{L} \cup \mathbb{B}_+$, $\mathcal{I}_+ \in \mathcal{F}(\mathbb{L}_+)$, $\theta_+ \in \Theta_+$, where Θ_+ denotes the association map space at time $k+1$, and

$$\bar{\omega}_{\mathcal{Z}_+}^{(\mathcal{I},\xi,\mathcal{I}_+,\theta_+)} = \omega^{(\mathcal{I},\xi)}\omega_{\mathcal{Z}_+}^{(\mathcal{I},\xi,\mathcal{I}_+,\theta_+)}, \tag{12}$$

$$\begin{aligned} w_{\mathcal{Z}_+}^{(\mathcal{I},\xi,\mathcal{I}_+,\theta_+)} = & 1_{\Theta_+(\mathcal{I}_+)}(\theta+)[1-\bar{P}_S^{(\xi)}]^{\mathcal{I}-\mathcal{I}_+}[\bar{P}_S]^{\mathcal{I}\cap\mathcal{I}_+} \\ & [1-r_{B,+}^{(\cdot)}]^{(\mathbb{B}_+-\mathcal{I}_+)} r_{B,+}^{(\mathbb{B}_+\cap\mathcal{I}_+)}[\bar{\psi}_{\mathcal{Z}_+}^{(\xi,\theta_+)}]^{\mathcal{I}_+}, \end{aligned} \tag{13}$$

$$\bar{P}_S^{(\xi)}(l) = \langle p^{(\xi)}(\cdot, l), p_S(\cdot, l)\rangle, \tag{14}$$

$$\bar{\psi}_{Z_+}^{(\xi,\theta_+)}(l_+) = \langle \bar{p}_+^{(\xi)}(\cdot, l_+), \psi_{Z_+}^{(\theta_+(l_+))}(\cdot, l_+)\rangle, \tag{15}$$

where $\psi_{\mathcal{Z}_+}^{(\theta_+(l_+))}(\mathbf{m}_+, l_+) = \psi_{\mathcal{Z}_+}(\mathbf{m}_+, l_+; \theta_+)$ (see Eq.(5)), and

$$\begin{aligned} \bar{p}_+^{(\xi)}(\mathbf{m}_+, l_+) = & 1_{\mathbb{L}}(l_+) \\ & \times \frac{\langle p_S(\cdot, l_+)\delta_{(\cdot)}(\mathbf{m}_+), p^{(\xi)}(\cdot, l_+)\rangle}{\bar{P}_S^{(\xi)}(l_+)} \\ & + 1_{\mathbb{B}_+}(l_+)p_{B,+}(\mathbf{m}_+, l_+), \end{aligned} \tag{16}$$

$$p_{\mathcal{Z}_+}^{(\xi,\theta_+)}(\mathbf{m}_+, l_+) = \frac{\bar{p}_+^{(\xi)}(\mathbf{m}_+, l_+)\psi_{\mathcal{Z}_+}^{(\theta_+(l_+))}(\mathbf{m}_+, l_+)}{\bar{\psi}_{\mathcal{Z}_+}^{(\xi,\theta_+)}(l_+)} \tag{17}$$

where the notation + has been used to abbreviate the symbols at time $k+1$ and $r_{B,+}^{(l_+)}$ denotes the probability of birth of the landmark l_+. The spatial distribution of each birth landmark, $p_{B,+}(\mathbf{m}_+, l_+)$, is modelled as a Gaussian and hence the resultant δ-GLMB filter follows a Gaussian mixture representation, where the spatial distribution of each landmark in the map with label l in each hypothesis results in a mixture of Gaussians (see III-B for more details).

The idea behind the joint prediction/update approach using a Gibbs sampler is to generate a smaller number of highly probable hypotheses using existing hypotheses, probability of detection and probability of survival values of landmarks and the set of received measurements at time $k+1$. This prevents the generation of insignificant and contradicting hypotheses and drastically reduces the computational complexity compared to the traditional prediction/update based δ-GLMB filter implementation [14] yielding a computationally efficient alternative for real-time implementations.

F. Trajectory estimation

Similar to PHD-SLAM in [3], the robot trajectory posterior is factorised as follows,

$$\begin{aligned} & p_{k|k}(\mathbf{x}_{1:k}|\mathcal{Z}_{1:k}, \mathbf{u}_{1:k}, \mathbf{x}_0) \\ & = \frac{g_{k|k-1}(\mathcal{Z}_k|\mathcal{Z}_{k-1}, \mathbf{x}_{0:k})p_{k|k-1}(\mathbf{x}_k|\mathbf{x}_{1:k-1}, \mathcal{Z}_{1:k-1}, \mathbf{u}_{1:k}, \mathbf{x}_0)}{p(\mathcal{Z}_k|\mathcal{Z}_{k-1}, \mathbf{u}_{1:k}, \mathbf{x}_0)} \\ & \times p_{k-1|k-1}(\mathbf{x}_{1:k-1}|\mathcal{Z}_{1:k-1}, \mathbf{u}_{1:k-1}, \mathbf{x}_0), \end{aligned} \tag{18}$$

and to cater for non-linear and non-Gaussian motion we adopt a Rao-Blackwellised particle filter [23] as explained in the section III-A.

III. Implementation

This section presents the implementation details of the proposed δ-GLMB-SLAM algorithm. The robot trajectory is propagated using a Rao-Blackwellised particle filter to cater for non-linear and possibly multimodal motion models in both 2D and 3D environments. The trajectory dependant landmark map is modeled as a labeled RFS and propagated using a δ-GLMB filter [16].

The δ-GLMB distribution of the landmark map posterior at time k can be approximated using a set of H highest probable hypotheses in the following form,

$$p(\mathcal{M}|\mathbf{x}_{0:k}) = \Delta(\mathcal{M})\sum_{h=1}^{H}\omega^{(h)}\delta_{\mathcal{I}^{(h)}}(\mathcal{L}(\mathcal{M}))\left[p^{(h)}\right]^{\mathcal{M}}, \tag{19}$$

where the right hand side of the above equation can also be represented as a parameter set of the form $\left\{(\mathcal{I}^{(h)}, \omega^{(h)}, p^{(h)})\right\}_{h=1}^{H}$, where for each hypothesis h, $\mathcal{I}^{(h)}$ represents a set of landmark labels, $\omega^{(h)}$ represents the probability of the hypothesis and $p^{(h)}$ consists of the spatial distribution $p^{(h)}(\mathbf{m}, l)$ of each landmark within this hypothesis.

Suppose that the robot trajectory posterior, $p_{k|k}(\mathbf{x}_{1:k}|\mathcal{Z}_{1:k}, \mathbf{u}_{1:k}, \mathbf{x}_0)$ can be represented by a set of weighted particles of the form $\Omega_k = \left\{w_k^{[i]}, \mathbf{x}_{1:k}^{[i]}\right\}_{i=1}^{N_s}$, where $w^{[i]}$ represents the weight of the particle i. Then, SLAM posterior (1) can be represented as,

$$\left\{w_k^{[i]}, \mathbf{x}_{1:k}^{[i]}, \left\{(\mathcal{I}^{(i,h)}, \omega^{(i,h)}, p^{(i,h)})\right\}_{h=1}^{H}\right\}_{i=1}^{N_s}, \tag{20}$$

978-1-5386-6020-1/18/$31.00 ©2018 IEEE

since the δ-GLMB distribution of the landmark map is conditioned on the robot trajectory. The details on the implementation of the particle filter and the Gaussian mixture (GM) implementation of the δ-GLMB filter is presented in the following sub-sections.

A. Robot trajectory estimation

Assume that the weighted set of particles Ω_{k-1} represent the robot trajectory posterior at time $k-1$. Then at time k, a new robot pose is sampled from each particle by applying the control commands as follows,

$$\mathbf{x}_k^{[i]} \sim f_{\mathbf{x}}(\mathbf{x}_k|\mathbf{x}_{k-1}^{[i]}, \mathbf{u}_k). \tag{21}$$

The new robot pose, $\mathbf{x}_k^{[i]}$, is then added to the set of particles Ω_{k-1}, creating a temporary set of particles distributed according to the proposal distribution given by,

$$\begin{aligned} &q_{k|k}(\mathbf{x}_{1:k}^{[i]}|\mathcal{Z}_{1:k-1}, \mathbf{u}_{1:k}, \mathbf{x}_0) \\ &= q_{k|k-1}(\mathbf{x}_k^{[i]}|\mathbf{x}_{1:k-1}^{[i]}, \mathcal{Z}_{1:k-1}, \mathbf{u}_{1:k}, \mathbf{x}_0) \\ &\times q_{k-1|k-1}(\mathbf{x}_{1:k-1|1:k-1}^{[i]}|\mathcal{Z}_{1:k-1}, \mathbf{u}_{1:k-1}, \mathbf{x}_0), \end{aligned} \tag{22}$$

where the transition density in the proposal distribution (Eq.(22)) is chosen to be equivalent to that of the robot trajectory posterior (Eq.(18)) as,

$$\begin{aligned} &q_{k|k-1}(\mathbf{x}_k^{[i]}|\mathbf{x}_{1:k-1}^{[i]}, \mathcal{Z}_{1:k-1}, \mathbf{u}_{1:k}, \mathbf{x}_0) \\ &= p_{k|k-1}(\mathbf{x}_k^{[i]}|\mathbf{x}_{1:k-1}^{[i]}, \mathcal{Z}_{1:k-1}, \mathbf{u}_{1:k}, \mathbf{x}_0). \end{aligned} \tag{23}$$

Now, each particle in the temporary set is assigned an importance weight given by,

$$\begin{aligned} w_k^{[i]} &= \frac{p_{k|k}(\mathbf{x}_{1:k}^{[i]}|\mathcal{Z}_{1:k}, \mathbf{u}_{1:k}, \mathbf{x}_0)}{q_{k|k}(\mathbf{x}_{1:k}^{[i]}|\mathcal{Z}_{1:k-1}, \mathbf{u}_{1:k}, \mathbf{x}_0)} \\ &\propto g_{k|k-1}(\mathcal{Z}_k|\mathcal{Z}_{1:k-1}, \mathbf{x}_{0:k}^{[i]}) w_{k-1}^{[i]}, \end{aligned} \tag{24}$$

where $g_{k|k-1}(\mathcal{Z}_k|\mathcal{Z}_{1:k-1}, \mathbf{x}_{0:k})$ is the normalisation constant in the δ-GLMB filter posterior given by,

$$g_{k|k-1}(\mathcal{Z}_k|\mathcal{Z}_{1:k-1}, \mathbf{x}_{0:k}) = \sum_{\mathcal{I},\xi,\mathcal{I}_+,\theta_+} \bar{\omega}_{\mathcal{Z}_+}^{(\mathcal{I},\xi,\mathcal{I}_+,\theta_+)}. \tag{25}$$

The importance weight of each particle in the temporary set is normalised such that, $\sum_{i=1}^{N_s} w_k^{[i]} = 1$. Then, a new set of N_s particles are drawn with replacement, where each particle is sampled with a probability proportional to its importance weight. The resultant particle set with its importance weights, denoted by Ω_k, represents the robot trajectory posterior density at time k.

B. Map estimation

In this section, we briefly summarize the details of the Gaussian mixture implementation of the δ-GLMB filter used in the estimation of the landmark map. Let $\mathcal{N}(.,\mu,\mathbf{P})$ denote a Gaussian probability density function with mean μ and covariance $\mathbf{P}$, and assume that the probability of detection of a landmark within the sensor FOV is of the form $p_D = p_D(\mathbf{m}, l)$. Let the observation model be a non-linear function of the form,

$$\mathbf{z}_k = h_k(\mathbf{m}_k, \mathbf{l}_k, \mathbf{x}^{[i]}{}_k, \nu_k), \tag{26}$$

where ν_k represents a zero-mean Gaussian measurement noise source with covariance $\mathbf{R}_k$ and $\mathbf{x}^{[i]}$ is the robot pose according to particle i. Then, assuming that the spatial distribution of $(\mathbf{m}_k, l_k)$ is of the form $\mathcal{N}(\mathbf{m}_k; \mu_k, \mathbf{P}_k)$, the measurement likelihood can be approximated as a Gaussian distribution by linearising:

$$\begin{aligned} &g_k(\mathbf{z}|\mathbf{m}_k, l_k, \mathbf{x}^{[i]}{}_k) \\ &\approx \mathcal{N}(\mathbf{z}; h_k(\mu_k, l_k, \mathbf{x}^{[i]}{}_k, 0), \mathbf{U}_k \mathbf{R}_k \mathbf{U}_k{}^T + \mathbf{H}_k \mathbf{P}_k \mathbf{H}_k{}^T), \end{aligned} \tag{27}$$

where $\mathbf{U}_k$ is the Jacobian of $h_k(\mathbf{m}_k, \mathbf{l}_k, \mathbf{x}^{[i]}{}_k, \nu_k)$ with respect to ν_k at $\nu_k = 0$ and $\mathbf{H}_k$ denotes the Jacobian of $h_k(\mathbf{m}_k, l_k, \mathbf{x}^{[i]}{}_k, 0)$ with respect to $\mathbf{m}_k$, at $\mathbf{m}_k = \mu_k$.

Furthermore, assume that the RFS $\mathcal{Q}_+$ of newly appearing features in the sensor FOV can be modelled by a labelled multi-Bernoulli distribution given by,

$$f_B(\mathcal{Q}_+) = \{r_{B,+}^{(l_+)}, p_{B,+}(\mathbf{m}_+, l_+|\mathbf{z}_+)\}_{l_+=1}^{|\mathcal{Z}_+|}, \tag{28}$$

where, $r_{B,+}^{(l_+)}$ denotes the probability of birth of landmark l_+, and its spatial distribution $p_{B,+}(\mathbf{m}_+, l_+|\mathbf{z}_+)$ is modelled as a Gaussian distribution (or a mixture of Gaussian distributions) using the adaptive birth approach proposed in [15]. Assume that each hypothesis of the landmark map distribution $p(\mathcal{M})$ (Eq.(10)) at time k is represented by the hypothesis weight $\omega^{(\mathcal{I},\xi)}$ and the set of spatial distributions of each landmark in the set $\mathcal{I}$ with label l is given by a mixture of weighted Gaussian distributions as,

$$p^{(\xi)}(\mathbf{m}, l) = \sum\nolimits_{j=1}^{J^{(\xi)}(l)} \alpha_j^{(\xi)} \mathcal{N}(\mathbf{m}; \mu_j^{(\xi)}(l), \mathbf{P}_j^{(\xi)}(l)), \tag{29}$$

where, $\alpha_j^{(\xi)}$ denotes the weight of j^{th} Gaussian component. Then, using Eq.(15)-(17) it can be shown that the measurement updated spatial density for a given association map θ_+ in the measurement updated δ-GLMB distribution (Eq.(11)) also results in a mixture of weighted Gaussian distributions of the form,

$$p_{\mathcal{Z}_+}^{(\xi,\theta_+)}(\mathbf{m}, l) = \sum\nolimits_{j=1}^{J^{(\xi)}(l)} \alpha_{\mathcal{Z}_+,j}^{(\xi,\theta_+)} \mathcal{N}(\mathbf{m}; \mu_{\mathcal{Z}_+,j}^{(\xi,\theta_+)}(l), \mathbf{P}_{\mathcal{Z}_+,j}^{(\xi,\theta_+)}(l)), \tag{30}$$

where $\alpha_{\mathcal{Z}_+,j}^{(\xi,\theta_+)}$, $\mu_{\mathcal{Z}_+,j}^{(\xi,\theta_+)}(l)$ and $\mathbf{P}_{\mathcal{Z}_+,j}^{(\xi,\theta_+)}(l)$ denote the weight, mean and covariance of the measurement updated j^{th} Gaussian distribution component using the association map θ_+. The weight $\bar{\omega}_{\mathcal{Z}_+}^{(\mathcal{I},\xi,\mathcal{I}_+,\theta_+)}$ of each hypothesis can be obtained using Eq.(12)-(16). Note that the sum of the hypothesis weights, is equivalent to the normalisation constant of the δ-GLMB update posterior (Eq.(11)), and is used in the trajectory update step in Section III-A.

In order to extract the landmark map, the cardinality distribution component of the δ-GLMB distribution of the landmark map of the highest weighted particle is obtained using its hypothesis weights. The highest weighted hypothesis component with the cardinality equivalent to the maximum a

978-1-5386-6020-1/18/$31.00 ©2018 IEEE

posteriori (MAP) cardinality estimate (see [14]) contains the labels and the mean locations of the landmarks in the map.

IV. Results

The performance of the proposed δ-GLMB-SLAM algorithm is evaluated using a set of Matlab simulations and compared with an efficient variant of LMB-SLAM using the recently proposed fast implementation of the LMB filter with Gibbs sampler [24]. Standard measurement gating approaches are used in both algorithms with identical parameters to reduce the computational costs. However we opt out of using measurement clustering in LMB-SLAM and instead we use parallelization at the particle level (using the Matlab parallel computing toolbox) in both algorithms. Birth features (newly appearing) are modeled using the adaptive birth approach [20] and a birth probability value of 0.01 is used with measurements that are not associated to any existing feature and a probability value of 0.005 is used if a measurement can be associated with at least one existing feature.

A robot is driven on a pre-planned path in a simulated environment consisting of 23 landmarks. The control commands and measurements are generated from a single run of the robot with added Gaussian noise according to the parameters in the Table. I and measurement clutter is generated with four separate runs with rates λ_c 1, 5, 10 and 15 points per scan. The probability of detection p_D of a landmark within the sensor FOV was set to 0.7 and the p_D of a landmark (already existing in the map) out of the FOV is set to 0. The probability of survival p_S of a feature within the sensor FOV is set to 0.95 and p_S of a landmark (already existing in the map) and out of the current sensor FOV is set to 1. These settings make sure that a landmark in the estimated map remains in the map when it leaves the current sensor FOV, which is consistent with the assumption that the landmarks remain static. A pruning threshold value of 0.08 is chosen in LMB-SLAM to prune insignificant features, and a hypothesis pruning threshold of 0.00001 is chosen in δ-GLMB-SLAM to remove insignificant hypotheses. These values produce comparable estimation results and were chosen by executing the simulations (without control noise and measurement clutter) multiple times with LMB-SLAM and δ-GLMB-SLAM under all four clutter conditions.

Both algorithms are executed with 15 Monte Carlo (MC) runs per each clutter rate. The estimated and actual robot trajectory of a sample MC run under each clutter rate is shown in Fig. 1. It can be seen that both algorithms produce almost identical results at low clutter rates, however, under high clutter, LMB-SLAM produce inferior results with multiple false features and drift in the trajectory estimate compared to δ-GLMB-SLAM. Root mean squared (RMS) robot pose estimation error in X, Y and heading angle are compared in Fig.2, Fig.3 and Fig.4 respectively. It is clear that δ-GLMB-SLAM produces smaller average pose estimation errors compared to LMB-SLAM in all clutter conditions (except λ_c=1). It can also be seen that LMB-SLAM produces inferior results during loop closure as the clutter rate increases yielding drifts in Y and heading angle. A comparison of the estimated feature map against the actual ground truth map is compared in terms of average OSPA distance in Table. II, and it is clear that even at the highest clutter rate, the average OSPA error of δ-GLMB-SLAM is smaller than that of LMB-SLAM. The average running time is compared in Table.III, and it is clear that the running time increases significantly with the clutter rate in LMB-SLAM compared to δ-GLMB-SLAM. These results are consistent with the fact that, LMB-SLAM expands its LMB distribution into a δ-GLMB distribution prior to measurement update and combines the resultant hypotheses after the update step. In comparison, δ-GLMB-SLAM retains the hypotheses until further measurement updates invalidate insignificant hypotheses, which results in a significantly robust performance in terms of pose estimation accuracy, OSPA distance and running time compared to LMB-SLAM.

TABLE I: Parameters Used in the Simulation

Robot/Sensor Parameters		Values
Velocity	v	1m/s
Sensor FOV	Range (r)	0 - 3m
	Bearing (b)	$-\pi$ - $+\pi$
Control Noise	Velociy (σ_v)	0.1m/s
	Steering Angle (σ_a)	2^0
Measurement Noise	Range (σ_r)	0.3m
	Bearing (σ_b)	2^0

TABLE II: Comparison of average OSPA distance (in meters) with standard deviation, with cut-off (c) value of 0.5 and the order (p) of 1.

Clutter (λ_c)	LMB-SLAM	δ-GLMB-SLAM
1	0.160 $\pm$ 0.035	0.114 $\pm$ 0.024
5	0.172 $\pm$ 0.031	0.095 $\pm$ 0.030
10	0.150 $\pm$ 0.033	0.113 $\pm$ 0.037
15	0.228 $\pm$ 0.052	0.114 $\pm$ 0.044

TABLE III: Comparison of average run time per step (in seconds) with standard deviation.

Clutter (λ_c)	LMB-SLAM	δ-GLMB-SLAM
1	1.042 $\pm$ 0.258	0.758 $\pm$ 0.127
5	1.301 $\pm$ 0.318	0.804 $\pm$ 0.112
10	1.503 $\pm$ 0.380	0.957 $\pm$ 0.143
15	1.558 $\pm$ 0.509	1.166 $\pm$ 0.168

V. Conclusion

In this paper, we have presented a new RFS based SLAM algorithm called δ-GLMB-SLAM. Similar to earlier RFS based SLAM algorithms, δ-GLMB-SLAM factorizes the SLAM posterior into the landmark map posterior and robot trajectory posterior via Rao-Blackwellization. The robot trajectory is propagated using a particle filter, and the landmark map is estimated using an efficient variant of the δ-GLMB filter based on Gibbs sampling. The performance of δ-GLMB-SLAM is evaluated using a series of simulations, and compared to the LMB-SLAM algorithm with a Gibbs sampling based joint map prediction and update approach. From the simulation results, it can be seen that the proposed δ-GLMB-SLAM algorithm

978-1-5386-6020-1/18/$31.00 ©2018 IEEE

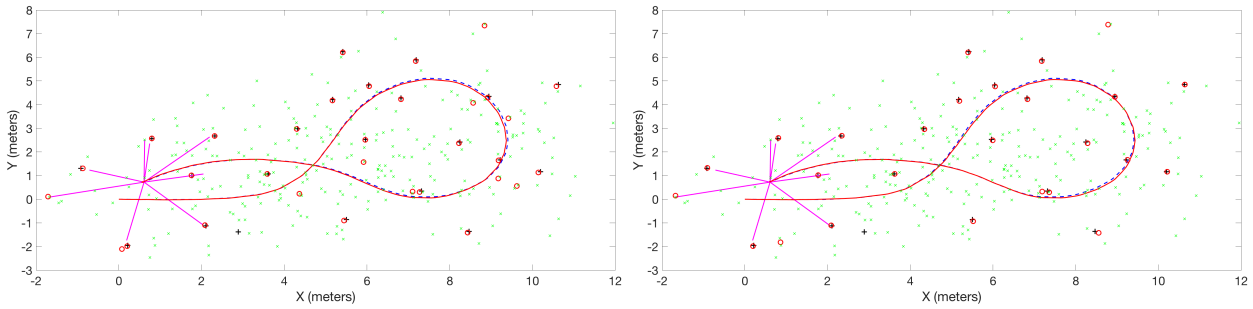

(a) LMB-SLAM [$\lambda_c = 1$] (b) δ-GLMB-SLAM [$\lambda_c = 1$]

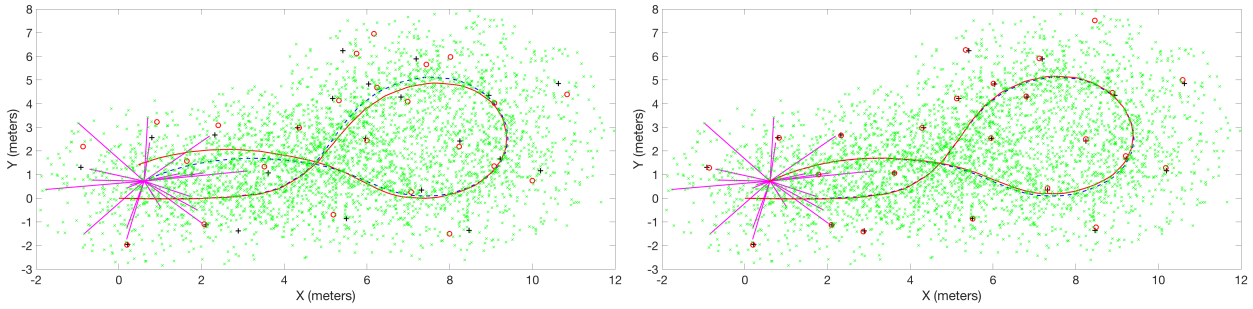

(c) LMB-SLAM [$\lambda_c = 15$] (d) δ-GLMB-SLAM [$\lambda_c = 15$]

Fig. 1: A comparison of the estimated robot trajectory (in red) superimposed on the ground truth robot trajectory (in dashed blue) for varying clutter conditions. The black plus signs represent the actual feature positions and the red circles represent the estimated feature positions. The green crosses represent accumulated measurement clutter and the magenta lines corresponds to feature observations.

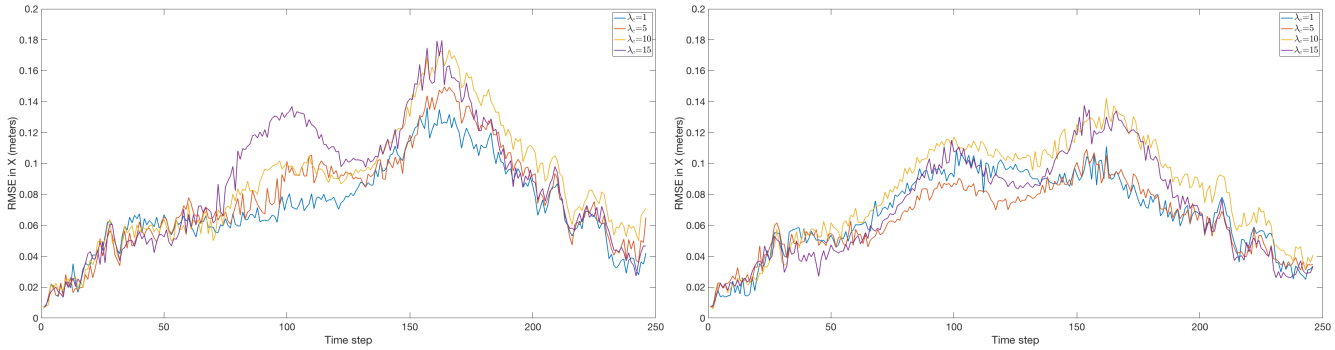

(a) LMB-SLAM (b) δ-GLMB-SLAM

Fig. 2: Comparison of RMSE in the X direction under varying clutter rates.

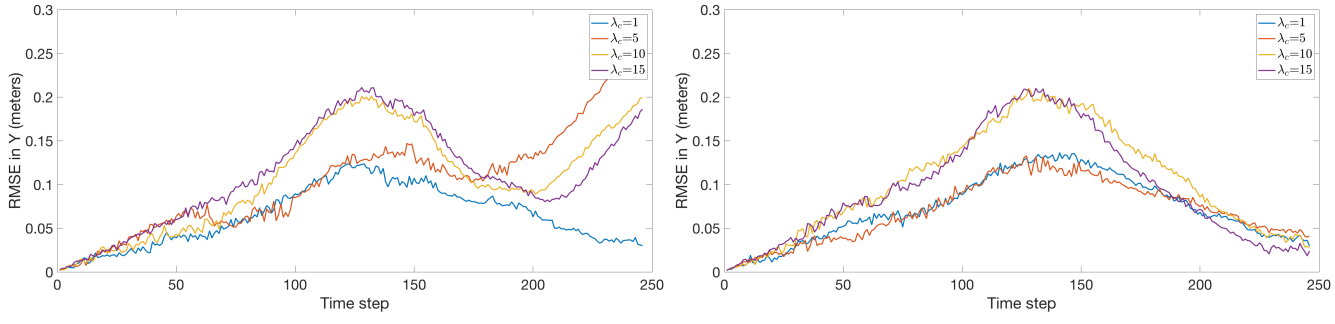

(a) LMB-SLAM (b) δ-GLMB-SLAM

Fig. 3: Comparison of RMSE in the Y direction under varying clutter rates.

978-1-5386-6020-1/18/$31.00 ©2018 IEEE

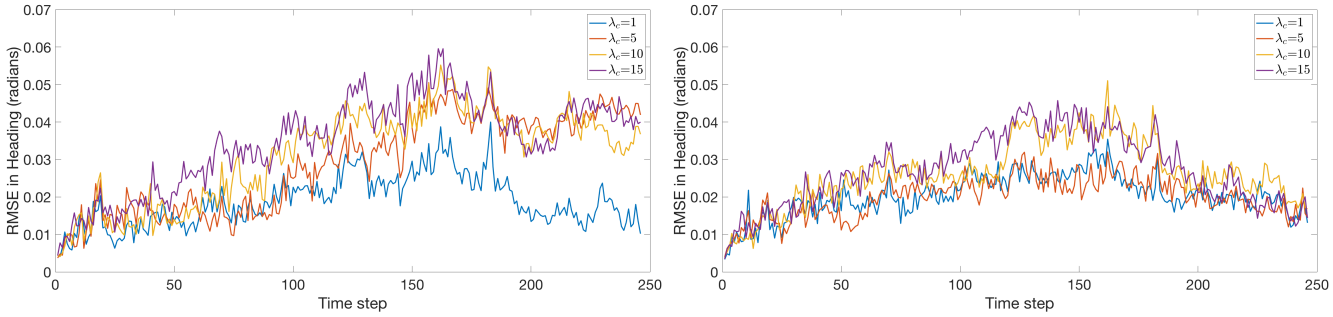

(a) LMB-SLAM (b) δ-GLMB-SLAM

Fig. 4: Comparison of RMSE in the heading under varying clutter rates.

outperforms LMB-SLAM in terms of pose estimation error, quality of the map and running time under varying clutter conditions. The quality of the pose estimation error and the map can be attributed to the fact that the δ-GLMB filter maintains multiple hypotheses for the landmark map state and removes insignificant hypotheses as further measurements invalidate contradicting hypotheses. LMB-SLAM however, combines multiple hypotheses during the measurement update step into a single LMB distribution resulting in a loss of information and drifts during loop closure. Standard measurement gating, particle level parallelization and Gibbs sampler based hypothesis generation result in a lower run time performance of δ-GLMB-SLAM, which outweighs the savings expected by combining multiple hypotheses in LMB-SLAM.

VI. Acknowledgements

This material is based upon work supported by the US Air Force Office of Scientific Research, under award number FA9550-17-1-0386. This work is also funded by the Advanced Mining Technology Center (AMTC) of Universidad de Chile and Conicyt-Fondecyt project 1150930.

References

[1] R. C. Smith and P. Cheeseman, "On the Representation and Estimation of Spatial Uncertainty," *The International Journal of Robotics Research*, vol. 5, no. 4, pp. 56–68, Dec. 1986.

[2] M. W. M. G. Dissanayake, P. Newman, S. Clark, H. F. Durrant-Whyte, and M. Csorba, "A solution to the simultaneous localization and map building (SLAM) problem," *IEEE Transactions on Robotics and Automation*, vol. 17, no. 3, pp. 229–241, 2001.

[3] M. Montemerlo, S. Thrun, D. Koller, and B. Wegbreit, "FastSLAM: A factored solution to the simultaneous localization and mapping problem," *Aaai/iaai*, 2002.

[4] S. Thrun, Y. Liu, D. Koller, A. Y. Ng, Z. Ghahramani, and H. Durrant-Whyte, "Simultaneous localization and mapping with sparse extended information filters," in *International Journal of Robotics Research*. Carnegie Mellon University, Pittsburgh, United States, Jul. 2004, pp. 693–716.

[5] F. R. Kschischang, B. J. Frey, and H. A. Loeliger, "Factor graphs and the sum-product algorithm," *IEEE Transactions on Information Theory*, vol. 47, no. 2, pp. 498–519, Jan. 2001.

[6] S. Thrun and M. Montemerlo, "The graph SLAM algorithm with applications to large-scale mapping of urban structures," in *International Journal of Robotics Research*. Stanford University, Palo Alto, United States, May 2006, pp. 403–429.

[7] F. Dellaert and M. Kaess, "Square Root SAM - Simultaneous Localization and Mapping via Square Root Information Smoothing." *I. J. Robotics Res.*, vol. 25, no. 12, pp. 1181–1203, 2006.

[8] C. Cadena, L. Carlone, H. Carrillo, Y. Latif, D. Scaramuzza, J. Neira, I. Reid, and J. J. Leonard, "Past, Present, and Future of Simultaneous Localization and Mapping: Toward the Robust-Perception Age," *IEEE Transactions on Robotics*, vol. 32, no. 6, pp. 1309–1332, 2016.

[9] R. Mahler, *Statistical Multisource-Multitarget Information Fusion*. Norwood, MA: Artech House, 2007.

[10] D. J. Daley and D. Vere-Jones, *An Introduction to the Theory of Point Processes*, ser. Probability and Its Applications. New York, NY: Springer New York, 2008.

[11] R. P. S. Mahler, "Multitarget bayes filtering via first-order multitarget moments," *IEEE Transactions on Aerospace and Electronic Systems*, vol. 39, no. 4, pp. 1152–1178, Oct. 2003.

[12] R. Mahler, "PHD filters of higher order in target number," *IEEE Transactions on Aerospace and Electronic Systems*, vol. 43, no. 4, pp. 1523–1543, Oct. 2007.

[13] B.-T. Vo and B.-N. Vo, "Labeled random finite sets and multi-object conjugate priors," *IEEE Transactions on Signal Processing*, vol. 61, no. 13, pp. 3460–3475, Jun. 2013.

[14] B.-N. Vo, B.-T. Vo, and D. Phung, "Labeled Random Finite Sets and the Bayes Multi-Target Tracking Filter," *IEEE Transactions on Signal Processing*, vol. 62, pp. 6554–6567, Dec. 2014.

[15] S. Reuter, B.-T. Vo, B.-N. Vo, and K. Dietmayer, "The Labeled Multi-Bernoulli Filter," *IEEE Transactions on Signal Processing*, vol. 62, no. 12, pp. 3246–3260, Jun. 2014.

[16] B.-N. Vo, B.-T. Vo, and H. G. Hoang, "An Efficient Implementation of the Generalized Labeled Multi-Bernoulli Filter," *IEEE Transactions on Signal Processing*, vol. 65, no. 8, pp. 1975–1987, Jun. 2017.

[17] J. Mullane, B.-N. Vo, M. D. Adams, and W. S. Wijesoma, "A random set formulation for Bayesian SLAM," in *2008 IEEE/RSJ International Conference on Intelligent Robots and Systems, IROS*, Nanyang Technological University, Singapore City, Singapore. IEEE, Dec. 2008, pp. 1043–1049.

[18] J. Mullane, B.-N. Vo, and M. D. Adams, "Rao-Blackwellised PHD SLAM," in *2016 IEEE International Conference on Robotics and Automation (ICRA*, Nanyang Technological University, Singapore City, Singapore. IEEE, Aug. 2010, pp. 5410–5416.

[19] J. Mullane, B. N. Vo, M. D. Adams, and B. T. Vo, "A Random-Finite-Set Approach to Bayesian SLAM," *IEEE Transactions on Robotics*, vol. 27, no. 2, pp. 268–282, 2011.

[20] H. Deusch, S. Reuter, and K. Dietmayer, "The Labeled Multi-Bernoulli SLAM Filter," *IEEE Signal Processing Letters*, vol. 22, no. 10, pp. 1561–1565, Oct. 2015.

[21] D. Moratuwage, B.-N. Vo, and D. Wang, "Collaborative Multi-vehicle SLAM with moving object tracking," in *2013 IEEE International Conference on Robotics and Automation (ICRA)*. IEEE, 2013, pp. 5702–5708.

[22] S. Reuter, "Multi-object tracking using random finite sets." *Ph.D. dissertation, Ulm University, Ulm, Germany*, 2014.

[23] A. Doucet and A. M. Johansen, "A tutorial on particle filtering and smoothing: fifteen years later," in *The Oxford Handbook of Nonlinear Filtering*. Oxford Univ. Press, Oxford, 2011, pp. 656–704.

[24] S. Reuter, A. Danzer, M. Stuebler, A. Scheel, and K. Granström, "A fast implementation of the Labeled Multi-Bernoulli filter using gibbs sampling." *Intelligent Vehicles Symposium*, pp. 765–772, 2017.